01,07

Devitrification of amorphous alloy $Al_{87}Ni_6Nd_7$ under heat treatment

© P.A. Uzhakin, V.V. Chirkova, N.A. Volkov, G.E. Abrosimova

Osipyan Institute of Solid State Physics RAS,
Chernogolovka, Russia

E-mail: uzhakin@issp.ac.ru

Received October 10, 2023
Revised October 10, 2023
Accepted October 11, 2023

The structure and thermal effects of crystallization of amorphous alloy $Al_{87}Ni_6Nd_7$ have been investigated by X-ray diffraction and differential scanning calorimetry. It is shown that crystallization proceeds in three stages. The activation energy of three stages of crystallization of amorphous alloy $Al_{87}Ni_6Nd_7$ has been calculated. It is found that after the third stage of crystallization the structure of the alloy is fully crystalline and consists of crystals of Al, $Al_{11}Nd_3$ and a previously unknown phase.

Keywords: amorphous alloys, nanocrystalline alloys, thermal effects, activation energy, X-ray diffraction.

DOI: 10.61011/PSS.2024.01.57845.225

1. Introduction

For new technology development, new materials with good physical and chemical properties are required. Such materials include amorphous and nanocrystalline alloys [1–8]. Amorphous alloys are produced by melt quenching. During cooling at a rate of approx. 10^6 K/s, disordered melt structure is fixed and after solidification the alloy structure is amorphous. Properties of amorphous alloys differ considerably from the properties of their crystalline counterparts. Amorphous structure is metastable and crystallization occurs in heating and/or deformation. Depending on the alloy composition and treatment conditions (temperature, heating rate, type, temperature and rate of deformation), crystallization results in formation of different structures (single-phase and multiphase, coarse- and fine-crystalline, homogeneous, textured, etc.). Phase transformations from amorphous to equilibrium crystalline state generally consist of several stages, whereby metastable phases usually occur at the first stage [9,10]. Nanocrystals are formed at the first crystallization stage, nanocrystalline alloy structure consists of nanocrystals distributed in the amorphous matrix. Crystal size, morphology and distribution depend on the method of amorphous structure exposure. The properties of nanomaterials forming during crystallization of amorphous alloys often exceed the properties of similar amorphous and crystalline alloys [11,12].

Several methods of nanocrystalline structure formation in amorphous alloys are available [13–19]. Heat treatment is one of the main methods. Nanocrystals are formed in amorphous alloys during heat treatment by the primary crystallization reaction and the resulting nanocrystals have chemical composition other than that of the matrix. Nanocrystals are formed through the diffusive mechanism, the remaining amorphous matrix is enriched by refractory alloy components that facilitates stability improvement. Amorphous matrix of the modified compound that is maintained between nanocrystals stabilizes the nanocrystalline structure and prevents the growth and coalescence of resulting nanocrystals.

As noted above, many nanocrystalline alloys feature unique physical properties. Aluminum-based alloys [20–29] that have high strength together with low specific weight are one of the most promising amorphous-crystalline alloys [30–33]. Al-TM-RE group nanocrystalline alloys (TM is the transition metal, RE is the rare earth element) consist of aluminum nanocrystals and surrounding amorphous phase. Whilst nanocrystal size is usually equal to 20−25 nm, and the crystalline phase proportion is not higher than 23−25% [34]. It should be noted that nanocrystals in these alloys feature the absence of linear defects [35,36].

As noted above, physical properties and, in particular, mechanical properties of Al-TM-RE amorphous alloys depend significantly on the nanocrystalline structure that is formed in them: on the crystal size, morphology and crystalline phase proportion. Parameters of the structural component in the amorphous phase are, in turn, defined by the chemical analysis of alloys and treatment conditions. It has been found earlier that the best properties were achieved at some intermediate crystal size [37,38]. To achieve materials with optimum complex properties, it is important to identify the principles of nanocrystalline structure formation. Currently, multiple papers are devoted to the investigation of crystallization processes in amorphous Al-Ni-RE alloys containing La, Gd, Yb, Y. The purpose of this study is to investigate crystallization of another alloy from the group of interest — amorphous $Al_{87}Ni_6Nd_7$ alloy.

2. Materials and methods

An amorphous alloy with a nominal composition of $Al_{88}Ni_6Nd_6$ was produced in a form of ribbon by fast melt quenching on a fast-moving substrate. The cooling

rate was 10^6 K/s. The ribbon width is 12 mm and thickness is 20 μm. Composition of the resulting amorphous ribbon was controlled by the local X-ray spectral analysis using ZeissSupra 50VP scanning election microscope. Thermal behavior of phase transformations in transition from amorphous to crystalline state was measured by the calorimetry method using PerkinElmer DSC-7 differential scanning calorimeter. The measurements were carried out during constant-rate heating, heating rates were equal to 5, 10, 20 K/min. For investigation of phase transformations, the samples were heated in the calorimeter at a rate of 20 K/min. The crystallization activation energy was calculated by the Kissinger method [39]:

$$\ln\left(\frac{T^2}{\beta}\right) = \frac{E_a}{RT} + C,$$

where T is the peak onset temperature at the particular heating rate (K), β is the heating rate (K/min), E_a is the activation energy (kJ/mol), R is the gas constant (J/(mol · K)).

The structure of samples was examined on SIEMENS D-500 X-ray diffractometer using Co Kα-radiation. For spectra processing, dedicated software was used for smoothing, background correction, separation of overlapping peaks, etc.

3. Experimentals

As noted above, the alloy composition was controlled by the X-ray spectral analysis method. Figure 1 shows the composition variation curve recorded on the sample section length of 300 μm, alloy component data is listed in Table 1. Real composition of the amorphous ribbon differs slightly from the nominal composition. Component distribution on the ribbon length is homogeneous.

No reflections from crystalline phases were detected on the X-ray diffraction patterns of the prepared samples. Figure 2 shows the X-ray diffraction pattern of the initial amorphous $Al_{87}Ni_6Nd_7$ alloy (the main diffusion peak region). Crystallization processes were investigated with constant-rate heating. Figure 3 shows a DSC curve of the amorphous $Al_{87}Ni_6Nd_7$ alloy recorded at a heating rate of 20 K/min. The DSC curve has three peaks corresponding to three crystallization stages.

Table 1. Chemical composition of amorphous alloy samples after quenching

Element	at.%
Al K	86.89
Ni K	5.81
Nd L	7.30
Total	100

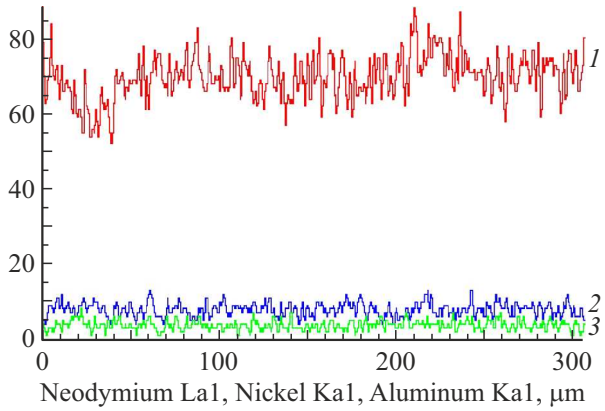

Figure 1. Distribution of $Al_{87}Ni_6Nd_7$ alloy components on the ribbon length: *1* — Al, *2* — Nd, *3* — Ni.

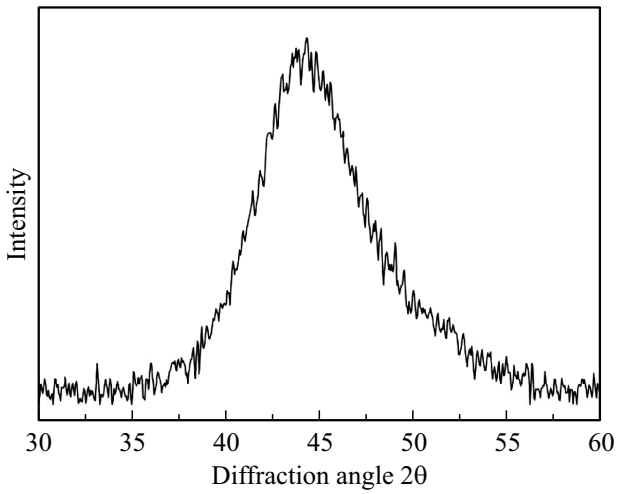

Figure 2. X-ray diffraction pattern of the initial amorphous $Al_{87}Ni_6Nd_7$ alloy.

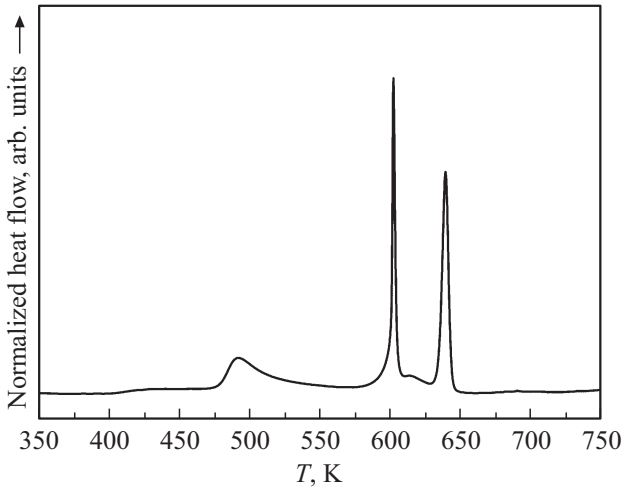

Figure 3. Thermogram of the amorphous $Al_{87}Ni_6Nd_7$ alloy at a heating rate of 20 K/min.

Table 2. Thermal characteristics of amorphous Al-Ni-(Nd, Y, La, Gd) alloys at a heating rate of 20 K/min: T_{cr} is the onset temperature of a particular crystallization stage; T_{peak} is the temperature of the peak top corresponding to a particular crystallization stage; ΔH is the thermal effect or heat release enthalpy of a particular crystallization stage

Composition	Crystallization stage 1			Crystallization stage 2			Crystallization stage 3			References
	T_{cr}, K	T_{peak}, K	ΔH, J/g	T_{cr}, K	T_{peak}, K	ΔH, J/g	T_{cr} K,	T_{peak}, K	ΔH, J/g	
$Al_{87}Ni_6Nd_7$	469	491	21.5	575	602	22.6	627	639	28.5	This study
$Al_{88}Ni_6Y_6$	443	460	41.4	576	598	40.0	610	623	39.2	[41]
$Al_{87}Ni_8La_5$	504	512	26.9	571	598	–	610	613	–	[42]
$Al_{87}Ni_8Gd_5$	474	487	26.2	605	606	39.0	631	635	53.5	[43]

Table 3. To the calculation of the activation energy of three crystallization stages of amorphous $Al_{87}Ni_6Nd_7$ alloy: β is the heating rate; T_{cr} is the crystallization onset temperature of each of the stages

Heating rate, β, K/min	Crystallization onset temperature, T_{cr}, K		
	Crystallization stage 1	Crystallization stage 2	Crystallization stage 3
5	461	567	613
10	465	571	620
20	469	575	627

The DSC curve (Figure 3) was used to determine the crystallization onset temperature and thermal effects for each crystallization stage. The crystallization onset temperature and thermal effect at the first stage are equal to 469 K and 21.5 J/g; at the second stage are 575 K and 22.6 J/g; at the third stage are 627 K and 28.5 J/g, respectively. A singularity associated with the glass transition point $T_g$was not observed on the heating curve. According to literature, some amorphous Al-TM-RE alloys do not have clearly pronounced T_g [40], and in some alloys of this system the glass transition temperature may coincide with the crystallization onset temperature [28]. Table 2, shows the known reference data on thermal characteristics of each crystallization stage of the amorphous Al-Ni-(Y, La, Gd) alloys with similar concentration composition (heating rate 20 K/min) [41–43]. It can be seen that thermal effects of three crystallization stages of the amorphous $Al_{87}Ni_6Nd_7$ alloy are much lower than those in alloys with other rare earth elements. However, the onset temperature of the first crystallization stage in the given amorphous $Al_{87}Ni_6Nd_7$ alloy is higher than that of the $Al_{88}Ni_6Y_6$ alloy and is significantly lower than in the $Al_{87}Ni_8La_5$ and $Al_{87}Ni_8Gd_5$ alloys.

The calorimetry data was used to calculate the crystallization activation energy of an amorphous alloy (Table 3). Activation energy was calculated as a slope of the line (Figure 4) through the experimental values plotted with $\ln(T^2/\beta)$ and $10^3/T_p$ as coordinates.

Activation energy E_a of the first, second and third crystallization stages is equal to 304, 460 and 306 kJ/mol,

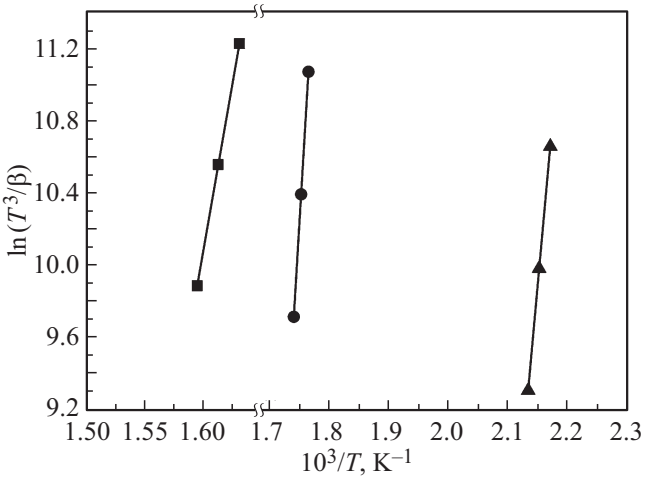

Figure 4. The Kissinger plot built to find the crystallization activation energy of the amorphous $Al_{87}Ni_6Nd_7$ alloy: triangles — crystallization stage 1; circles — crystallization stage 2; squares — crystallization stage 3.

respectively. The data obtained for the activation energy of the first crystallization stage of the amorphous $Al_{87}Ni_6Nd_7$ alloy is in good agreement with the data on the activation energy of Al-Ni-Nd alloys represented in [40]. Increase in the concentration of rare earth element Nd results in an increase in the activation energy of the first crystallization stage of amorphous Al-Ni-Nd alloys [40].

Table 4. Activation energy E_a of the first crystallization stage in the amorphous Al-Ni-(Nd, Dy, Gd, Sm, Y, Ce, La) alloys

Composition	E_a, kJ/mol	References
$Al_{87}Ni_8Dy_5$	163	[21]
$Al_{87}Ni_8Gd_5$	199	[21]
$Al_{87}Ni_7Sm_6$	260	[44]
$Al_{87}Ni_6Y_7$	283	[40]
$Al_{87}Ni_6Nd_7$	304	This study
$Al_{87}Ni_6Ce_7$	363	[40]
$Al_{87}Ni_7La_6$	311	[40]

For comparison with the alloy studied herein, Table 4 shows the activation energies of the first crystallization stage for Al-Ni-(Dy, Gd, Sm, Y, Ce, La) alloys. The activation energies of the amorphous Al-Ni-RE alloys whose composition differs from the alloy addressed herein by approx 1–2 at.% are taken from [21,40,44].

For phase composition modification in heating, samples were heated in the calorimeter at a rate of 20 K/min to temperatures corresponding to the end of each of the three crystallization stages. Figure 5 shows the X-ray diffraction pattern of the amorphous $Al_{87}Ni_6Nd_7$ alloy heated to 533 K (end of the first crystallization stage). Analysis of the X-ray diffraction pattern has shown that aluminum nanocrystals are formed at the first crystallization stage and after the end of the stage the alloy structure includes aluminum nanocrystals and remaining amorphous phase.

At the second crystallization stage (at about 613 K), $Al_{11}Nd_3$ crystals are formed (space group Immm), which corresponds to the equilibrium diagram of Al-Nd. After the end of the second crystallization stage, the structure contains

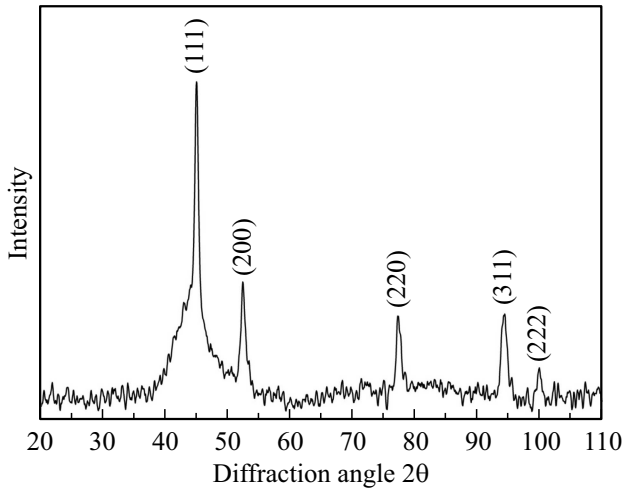

Figure 5. X-ray diffraction pattern of $Al_{87}Ni_6Nd_7$ alloy heated to 533 K (end of the first crystallization stage).

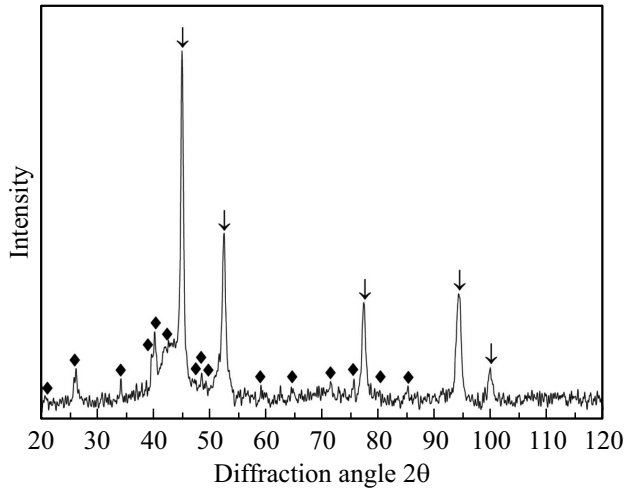

Figure 6. X-ray diffraction pattern of $Al_{87}Ni_6Nd_7$ alloy heated to 613 K (after the second crystallization stage): arrows — reflections from Al crystals; rhombuses — $Al_{11}Nd_3$.

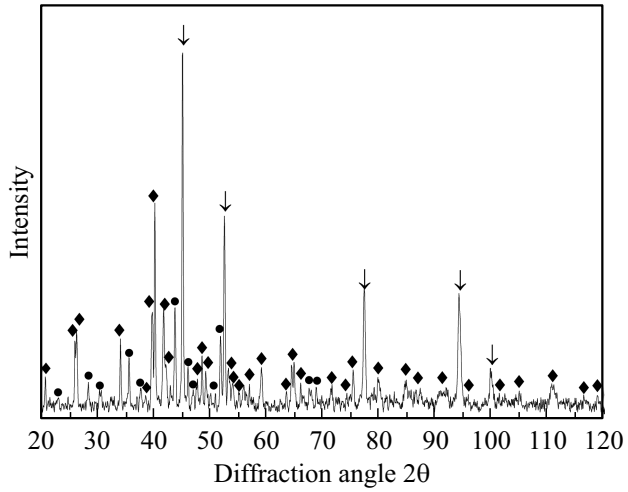

Figure 7. X-ray diffraction pattern of $Al_{87}Ni_6Nd_7$ alloy after the third crystallization stage: arrows — reflections from Al crystals; rhombuses — $Al_{11}Nd_3$; circles — unknown phase.

Al, $Al_{11}Nd_3$ crystals and a small amount of the remaining amorphous phase (Figure 6).

Figure 7 shows an X-ray diffraction pattern of the sample heated to the temperature corresponding to the end of the third crystallization stage. After this stage, the alloy structure is fully crystalline. The phase analysis has shown that after the third crystallization stage the X-ray diffraction pattern, besides the reflections from Al and $Al_{11}Nd_3$ crystals, also shows reflections of another previously unknown phase. Additional investigations are required to identify the structure of the new phase.

4. Conclusion

Crystallization of the amorphous $Al_{87}Ni_6Nd_7$ alloy with heat treatment was examined. It is shown that the

crystallization consists of three stages. Thermal effects of all three crystallization stages were defined; they are equal to 21.5, 22.6 and 28.5 J/g, respectively. The activation energy of the first crystallization stage (304 kJ/mol) was calculated. Thermal effects of the amorphous $Al_{87}Ni_6Nd_7$ alloy studied herein and of Al-Ni-RE alloys with other rare earth elements were compared.

A phase transformation sequence with heat treatment of the amorphous $Al_{87}Ni_6Nd_7$ alloy was identified. Aluminum crystals are formed at the first crystallization stage, $Al_{11}Nd_3$ phase crystals are formed at the second crystallization stage crystals of the previously unknown crystalline phase are formed at the third stage.

Acknowledgments

Authors are grateful to R.I. Usmanov for the differential scanning calorimetry testing.

Funding

This study was financially supported by the Russian Science Foundation, project No. 23-23-00171.

Conflict of interest

The authors declare that they have no conflict of interest.

References

[1] C. Morón, C. Cabrera, A. Morón, A. García, M. González. Sensors **15**, *11*, 28340 (2015). https://doi.org/10.3390/s151128340
[2] G. Herzer. Acta Mater. **61**, *3*, 718 (2013). http://dx.doi.org/10.1016/j.actamat.2012.10.040
[3] Y. Yoshizawa, S. Oguma, K. Yamauchi. J. Appl. Phys. **64**, 6044 (1988). http://dx.doi.org/10.1063/1.342149
[4] A. Aronin, G. Abrosimova. Metals **10**, 358, (2020). https://doi.org/10.3390/met10030358
[5] A. Inoue, M. Yamamoto, H.M. Kimura, T. Masumoto. J. Mater. Sci. Lett. **6**, 194 (1987). https://doi.org/10.1007/BF01728983
[6] A. Inoue. J. Mater. Sci. Lett. **43**, 365 (1998). https://doi.org/10.1201/9781420033816.ch3
[7] G.E. Abrosimova, A.S. Aronin, O.I. Barkalov, M.M. Dementieva. FTT **55**, *9*, 1773 (2013). (in Russian). https://doi.org/10.1134/S1063783413090023
[8] Z. Huo, G. Zhang, J. Han, J. Wang, S. Ma, H. Wang. Processes **10**, *6*, 1203 (2022). https://doi.org/10.3390/pr10061203
[9] S. Spriano, C. Antonione, R. Doglione, L. Battezzati, S. Cardoso, J.C. Soares, M.F. Da Silva. Phil. Mag. B **76**, *4*, 529 (1997). https://doi.org/10.1080/01418639708241119
[10] L.Q. Xing, J. Eckert, W. Löser, L. Schultz. Appl. Phys. Lett. **74**, *5*, 664(1999). https://doi.org/10.1063/1.122980
[11] V.V. Tchirkova, N.A. Volkov, I.A. Sholin, G.E. Abrosimova, A.S. Aronin. FTT **64**, *7*, 759 (2022). (in Russian). https://doi.org/10.21883/FTT.2022.07.52558.307
[12] S.P. Mondal, K.H. Maria, S.S. Sikder, S. Choudhury, D.K. Saha, M.A. Hakim. J. Mater. Sci. Technol. **28**, *1*, 21 (2012). https://doi.org/10.1016/S1005-0302(12)60018-8
[13] N.V. Ershov, Yu.P. Chernenkov, V.A. Lukshina, O.P. Smirnov, D.A. Shishkin. FTT **63**, *7*, 834 (2021). (in Russian). https://doi.org/10.21883/FTT.2021.07.51032.041
[14] R.J. Hebert, J.H. Perepezko, H. Rösner, G. Wilde. Beilstein J. Nanotechnol. **7**, 1428 (2016). https://doi.org/10.3762/bjnano.7.134
[15] G. Abrosimova, A. Aronin, D. Matveev, E. Pershina. Mater. Lett. **97**, 15 (2013). https://doi.org/10.1016/j.matlet.2013.01.092
[16] G.E. Abrosimova, A.S. Aronin. FTT **59**, *11*, 2227 (2017). (in Russian). https://doi.org/10.21883/FTT.2017.11.45066.142
[17] A. Aronin, D. Matveev, E. Pershina, V. Tkatch, G. Abrosimova. J. Alloys Compd. **715**, 176 (2017). https://doi.org/10.1016/j.jallcom.2017.04.305
[18] Zs. Kovács, P. Henits, S. Hóbor, Á. Révész. Rev. Adv. Mater. Sci. **18**, 593 (2008). https://doi.org/10.1016/J.SCRIPTAMAT.2006.02.004
[19] N.N. Sitnikov, A.V. Shelyakov, R.V. Sundeev, I.A. Khabibullina. FTT **62**, *5*, 644 (2020). (in Russian). https://doi.org/10.21883/FTT.2020.05.49223.14M
[20] Y.H. Kim, A. Inoue, T. Masumoto. Mater. Trans. JIM **32**, *4*, 331 (1991). https://doi.org/10.2320/matertrans1989.32.331
[21] T. Mika, M. Karolus, L. Boichyshyn, G. Haneczok, B. Kotur, V. Nosenko. Chem. Met. Alloys **5**, 50 (2012). https://doi.org/10.30970/cma5.0208
[22] M.Y. Na, K.C. Kim, W.T. Kim, D.H. Kim. Appl. Micro. **43**, *127* (2013). http://dx.doi.org/10.9729/AM.2013.43.3.127
[23] Z.C. Zhong, X.Y. Jiang, A.L. Greer. Phil. Mag. B **76**, *4*, 505 (1997). http://dx.doi.org/10.1080/01418639708241116
[24] T. Mika, M. Karolus, G. Haneczok, L. Bednarska, E. Łagiewka, B. Kotur. J. Non-Cryst. Solids **354**, *27*, 3099 (2008). https://doi.org/10.1016/j.jnoncrysol.2008.01.020
[25] M. Calin, U. Köster. Mater. Sci. Forum **269–272**, 749 (1998). https://doi.org/10.4028/www.scientific.net/MSF.269-272.749
[26] M.C. Gao, F. Guo, S.J. Poon, G.J. Shiflet. Mater. Sci. Eng. **485**, 532 (2008). https://doi.org/10.1016/j.msea.2007.08.009
[27] P. Rizzi, A. Habib, A. Castellero, L. Battezzati. Intermetallics **33**, 38–43 (2013). https://doi.org/10.1016/j.intermet.2012.09.026
[28] J. Zhang, P. Shi, A. Chang, T. Zhao, W. Lia, C. Chang, J. Jia, Q. Wang, F. You, D. Feng, X. Wang, Y. Zhao, Tao Li, Y. Huang, S. Ana. J. Non-Cryst. Solids X **1**, 100005 (2019). https://doi.org/10.1016/J.NOCX.2018.100005
[29] P. Rizzi, L. Battezzati. J. Alloys Compd. **434-435**, 36 (2007). https://doi.org/10.1016/j.jallcom.2006.08.186
[30] D.V. Louzguine, A. Inoue. J. Non-Cryst. Solids **311**, 281 (2002). https://doi.org/10.1016/S0022-3093(02)01375-3
[31] D.V. Louzguine-Luzgin, A. Inoue. J. Alloys Comp. **399**, *1–2*, 78 (2005). https://doi.org/10.1016/j.jallcom.2005.02.018
[32] A. Inoue, T. Ochiai, Y. Horio, T. Masumoto. Mater. Sci. Eng. **179-180**, 649 (1994). https://doi.org/10.1016/0921-5093(94)90286-0
[33] Y. He, Y.F. Poon, G.Y. Shiflet. Science. **241**, 1640 (1988). https://doi.org/10.1126/science.241.4873.1640
[34] G.E. Abrosimova, A.S. Aronin, Yu.V. Kir'janov, T.F. Gloriant, A.L. Greer. Nanostruct. Mater. **12**, 617620 (1999).
[35] G.E. Abrosimova, A.S. Aronin. FTT **44**, *6*, 961 (2002). (in Russian).

[36] G.E. Abrosimova, A.S. Aronin. FTT **51**, 9 (2009). (in Russian).
[37] K. Lu. Mater. Sci. Eng. **16**, *4*, 161 (2019). https://doi.org/10.1016/0927-796X(95)00187-5
[38] G. Herzer. Magn. Hysteresis Nov. Mater. **338**, 711 (1997). https://doi.org/10.1007/978-94-011-5478-9_77
[39] H.E. Kissinger. J. Res. Natl. Bur. Stand. **57**, *4*, 2712 (1956). https://doi.org/10.6028/jres.057.026
[40] Z.H. Huang, J.F. Li, Q.L. Rao, Y.H. Zhou. Mater. Sci. Eng. **489**, 380 (2008). https://doi.org/10.1016/j.msea.2007.12.027
[41] G.E. Abrosimova, A.S. Aronin. FTT **51**, 9 (2009). (in Russian).
[42] A. Aronin, D. Matveev, E. Pershina, V. Tkatch, G. Abrosimova. J. Alloys Compd. **715**, 176 (2017). https://doi.org/10.1016/j.jallcom.2017.04.305
[43] G. Abrosimova, V. Chirkova, E. Pershina, N. Volkov, I. Sholin, A. Aronin. Metals **12**, *2*, 332 (2022). https://doi.org/10.3390/met12020332
[44] L. Battezzati, P. Rizzi, V. Rontó. Mater. Sci. Engin. **375**–**377**, 927 (2002). https://doi.org/10.1016/j.msea.2003.10.042

Translated by E.Ilinskaya